

Height triangulation of artificial optical emissions in the F-layer

M. Ashrafi and M. J. Kosch

Department of Communications Systems, Lancaster University, Lancaster, LA1-4WA, UK

K. Kaila

Department of Physical Sciences, University of Oulu, Oulu, FIN-90570, Finland

Abstract.

Using the EISCAT high gain high frequency (HF) Heating facility located in northern Scandinavia (69.59° N, 19.23° E), HF-induced artificial auroral emissions can be produced at ionospheric F-region altitudes. On 12th November 2001, the EISCAT Heating facility, pumping with O-mode at 5.423 MHz and 550 MW effective radiative power (ERP), produced artificial optical rings which appeared immediately at pump-on and collapsed into blobs after ~ 60 s whilst descending in altitude. Observations were made using cameras in two different locations, one looking into the magnetic zenith over EISCAT recording in white-light, and the other pointing to the local zenith ~ 50 km from EISCAT in 630.0 and 557.7 nm (Skibotn, 69.35° N, 20.36° E). The altitudes of the initial optical ring and steady-state blob have been estimated by height triangulation. The change in height of all the optical structures during each Heater on cycle has been calculated using two-dimensional cross-correlation of the bi-static images. Consistent descent of the optical signature is similar to the lowering of other effects from ionospheric heating such as the EISCAT UHF radar ion line enhancements and stimulated electromagnetic emissions. We describe the details of the height triangulation technique used.

1 Introduction

Accelerated electrons resulting from ionospheric pumping with high frequency (HF) high power radio waves can cause excitation of the atomic oxygen and lead to the artificial green (557.7 nm) and red line (630.0 nm) emissions in the F layer. The phenomena has been observed at low and middle latitudes, for example at Arecibo (Sipler et al., 2001; Bernhardt et al., 1988, 1989), Platteville (Haslett and Megill, 1974) and in Russia at the SURA facility (Bernhardt et al., 1991), for a long time. There was no report of such observations at high latitudes until recently when observations of artificial optical emissions were made in Scandinavia and Alaska (Brändström et al., 1999; Kosch et al., 2000; Leyser et al., 2000; Pedersen and Carlson, 2001; Gustavsson et al., 2001). The phenomenon occurs at altitudes near the reflection height of the HF pump wave where electrons accelerated by HF-driven electrostatic waves to high energies propagate out of the interaction region up and down the magnetic field lines (Bernhardt et al., 1988). The accelerated electrons' energy is lost by inelastic collisions with the neutral atmosphere to excite neutrals such as the 1D and 1S states of atomic oxygen. The red-line emission at 630.0 nm and green-line emission at 557.7 nm are the two brightest stimulated optical emissions during ionospheric heating experiments which

result from inelastic collisions of accelerated electrons with energies higher than 1.96 eV and 4.17 eV, respectively. There have been several attempts in the past to estimate the height of the artificial optical emission (Brändström et al., 1999; Gustavsson et al., 2001). This is important in understanding the electron acceleration excitation mechanisms and accelerated electron energy spectrum resulting in the artificial aurora. In this paper we present observations of the ionospheric modification experiment on 12 November 2001 at the EISCAT Heating facility in northern Scandinavia and describe a triangulation technique using images from two cameras separated by ~ 50 km in order to estimate the height of the optical emission throughout the heating experiment.

2 Experimental observations

On 12th November 2001, the EISCAT Heater was transmitting O-mode waves at 5.423 MHz operating at 550 MW ERP with a 2 min. on, 2 min. off cycle with the pump beam pointed 9° south of vertical in the first half of the experiment (15:05 - 16:55 UT). During the second half (16:57 - 20:00 UT), the Heater beam was scanning between 3° and 15° south of vertical in 3° steps. The pump beam width is $\sim 7^\circ$ throughout and magnetic zenith is 12.8° south of vertical. Optical observations were made simultaneously from two stations ~ 50 km apart. The DASI (Digital All-Sky Imager) camera (Kosch et al., 1998) with a 50° field of view was located at Skibotn, Norway (69.35° N and 20.36° E), pointing vertically using narrow-band interference filters at 557.7 or 630.0 nm. The other camera situated at Ramfjordmoen (69.59° N and 19.23° E) was looking along the magnetic field line direction with a 50° field of view, recording in white light. DASI used an integration time of 5 s for 557.7 nm and 10 s for 630.0 nm whereas the Ramfjordmoen camera used a 13 seconds cycle. The optical signature produced by the pump waves was a ring shaped structure at the start of the Heater on period which collapsed into a blob after ~ 60 s

of heating. Intensities up to ~ 100 and ~ 300 Rayleighs in 630.0 nm were observed for the ring and blob structure artificial aurora, respectively. For details of the observation refer to Kosch et al. (2004).

3 Height triangulation method

Multi-station observations of auroral emissions and the application of height triangulation in estimating the location of the emission is a well known, long standing technique (Störmer, London, 1955). However, by knowing the special distribution of the emission region as additional information, computer tomography is another method used to estimate the height of the emissions (Solomon et al., 1984; Semeter et al., 1999; Gustavsson et al., 2001). Tomographic reconstruction generally requires more than two points of view, which were not available during our experiment. In our case, we have used the images from two optical stations at Skibotn and Ramfjordmoen to estimate the height of the artificial auroral emissions produced by the EISCAT high gain Heater. The green line data from the DASI camera together with the white light recordings of the Ramfjordmoen camera have been used to estimate the height of the emissions. We assume that the vertical extent of the artificial aurora is limited, or equivalently the height triangulation is focusing on the region of greatest intensity, i.e. near the bottom of the forms. The O(1 S) 557.7 nm emission is suitable for studying temporal variations, due to its short radiative lifetime (~ 0.7 s) compared to the brighter O(1 D) 630.0 nm emission with ~ 30 s effective lifetime in the F-layer (Gustavsson et al., 2001). In addition, the white light data from the Ramfjordmoen camera is dominated by the 557.7 nm emission because of the spectral response of the camera, therefore it is reasonable to compare the white light images with the DASI green line data.

Star field images, computed from a star catalogue and mapped down onto the data images, have been used to cor-

rect the lens distortion for both cameras (Duffet-Smith, Cambridge, 1990) and calculate each camera's exact position and pointing direction. An additional transformation has been applied to the Ramfjordmoen camera as it is pointing toward magnetic zenith over EISCAT (Azimuth 183° , Elevation 77.2°) and so it is not co-aligned with the line to the centre of the Earth, i.e. the spherical coordinate system origin. Second order corrections have been made in the image x and y directions in order to compensate for the discrepancies between the recorded images and the star map, i.e. lens distortion, which is typical for wide-aperture night-vision imaging systems. However, a better accuracy is achieved for more central image pixels rather than those close to the edge of the image. Since the optical structures are located mostly away from the edge of the field of view, there is no significant error introduced into the height triangulation. The same corrections have to be made to all the images from each camera.

In order to eliminate the effect of the unwanted background signal, which also includes the stars in case of the Ramfjordmoen camera recording in white light, background subtraction and filtering is required. Figure 1 shows the DASI and Ramfjordmoen camera images before (1-a) and after (1-b) filtering and background subtraction. By subtracting the average of five successive images before each Heater on cycle from any image during the same cycle, a clear picture of the artificial emissions is obtained (Fig. 1-b). In addition, a 5×5 median filter has been applied to the images to eliminate the background noise and residual stars due to their motion. The integration and cycle times of the cameras are different, therefore synchronization is required. The Ramfjordmoen camera images have been subjected to linear time interpolation in order to synchronize them with the DASI data. The difference in time between the real camera image and the required synchronized image is only a few seconds, therefore linear interpolation is a good approximation in order to produce the desired image. In addition, to perform the height triangulation, it is essential to have the synchronized

images in a common coordinate system. Geographic coordinates are well suited to this purpose. In order to perform this transformation, first the image is converted into altitude and azimuth angles or horizon coordinates. Then, by choosing a certain height, the image can be transformed to geographic coordinates. Figure 1-c shows the converted images in geographic coordinates for both cameras at 220 km altitude.

Finally, the linear 2-dimensional cross-correlation coefficient between the corresponding images in geographic coordinates from the different platforms has been calculated within a common geographic area between 17.3° and 20.2° in Longitude and 68.6° and 69.6° in Latitude. Figure 2 shows the superimposed images from the two cameras assuming three different heights. Panel (2-a) is for 320 km altitude, giving a cross-correlation of ~ 0.05 . Panel (2-b) is for the highest correlation of ~ 0.7 at 220 km. The ring-shaped structures of the artificial aurora from both cameras are perfectly overlapped. Panel (2-c) is for 170 km altitude with a correlation coefficient of ~ 0.1 . The best correlation is achieved for the height which is most likely to be the real height of the brightest part of the optical emission. At this height, the apparent horizontal overlap of the ring structure of the artificial aurora, observed from the two different platforms, is optimized. The cross-correlation coefficient has been calculated for a range of heights in the vicinity of the pump wave reflection altitude. Using EISCAT UHF radar electron density profiles, the reflection height of the Heater pump wave has been estimated, which is ~ 220 - 235 km for 15-17 UT (Kosch et al., 2004). The small circles in Figure 2 represent the projection of the magnetic field line at Ramfjordmoen in geographic coordinates. The corresponding height for each point has been marked in kilometers.

Figure 3 represents the height vs. cross-correlation coefficient for different intervals over one of the Heater on cycles starting at 16:57:00 UT which lasts for 2 minutes. The correlation coefficient vs. height is shown for 40, 60, 80 and 100 seconds after the Heater on from top to bottom, respec-

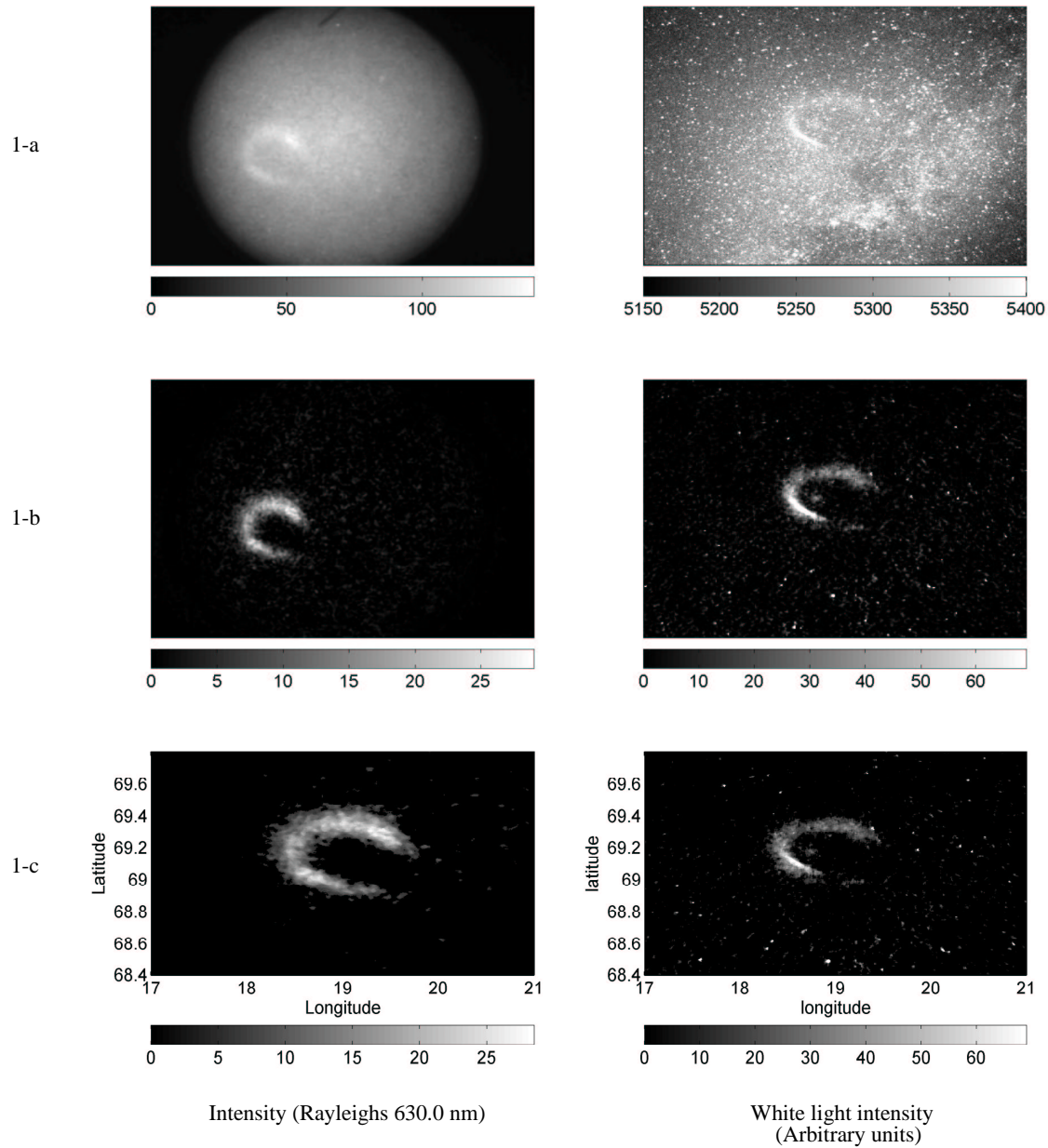


Fig. 1. The left column shows DASI images. From top to bottom is the raw, background subtracted and filtered image, and image projection into geographic coordinates for 220 km altitude. The images are calibrated in Rayleighs for 630.0 nm. The column on the right is the same sequence of images from the Ramfjordmoen camera in white light. In this case the red line emission data at 630.0 nm is used for demonstration purposes only and the height triangulation analysis has been applied to green line data at 577.7 nm..

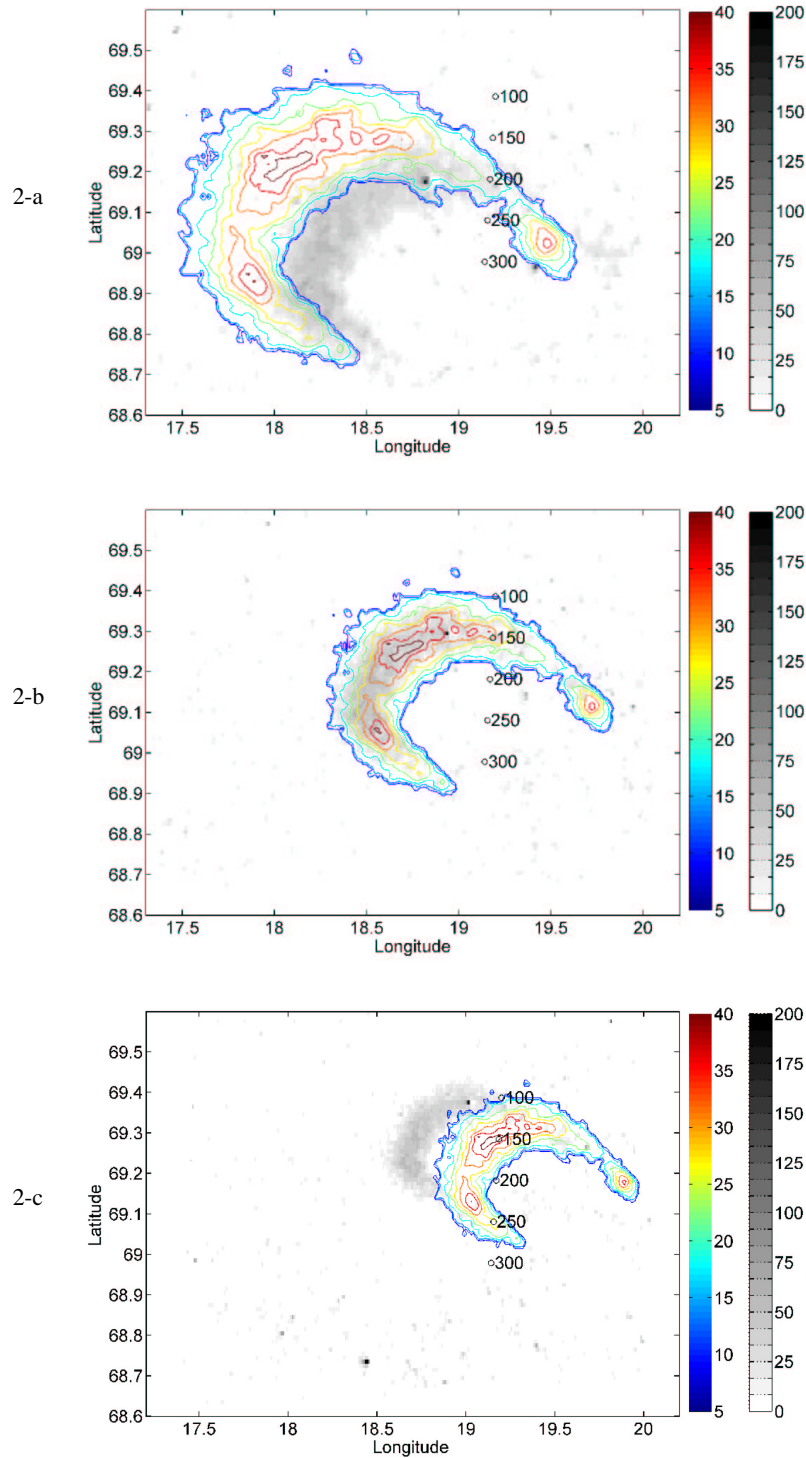


Fig. 2. Superimposed optical aurora from the DASI and Ramfjordmoen cameras at 16:25:10 UT projected in geographic coordinates assuming three different projection altitudes. The color contour plots are the optical annuli recorded by the DASI camera in green line emission (557.7 nm) overlaid on the gray scale images from the Ramfjordmoen camera in white light. Intensity is in arbitrary units. Panels a, b and c are for 320, 220 and 170 km altitudes, respectively. The small circles represent the projection of the magnetic field line through Ramfjordmoen for different altitudes.

tively. The points shown by asterixes are the corresponding cross-correlation coefficient for each two kilometer altitude step. The red curve is a second order polynomial fit to the points, the maximum of which is taken to be the maximum cross-correlation achieved for any given time. Therefore, the height of maximum correlation is considered to be the true equivalent height where the optical emissions come from assuming zero vertical extent. In the ideal case the cross-correlation for this altitude should be close to unity but considering the measurement uncertainty, lens distortion corrections, noise and other factors involved (e.g. vertical extent) this is not generally achievable.

The error associated with the height estimation is generated by uncertainties in the cross correlation, which is a result of height ambiguity or vertical extension, lens distortion, image noise, etc. and is expressed as the standard deviation of the correlation coefficient for each selected altitude. The uncertainty in height triangulation of the optical emission is obtained by simulation, i.e. the curve fit shown in Figure 3 is performed many times, varying the cross-correlation values for each selected altitude randomly within each value's standard deviation. The altitude error on average is ~ 4 -5 km.

4 Results and conclusion

The change in height of the brightest part of the optical emission has been calculated for Heater on cycles from 16:25 - 17:00 UT. Figure 4 shows the height triangulation results (asterixes) plotted on top of the EISCAT UHF radar backscatter power for 9 sequential Heater cycles. The intervals indicated by black lines show the Heater on cycles and the labels are radar zenith angles south of vertical. The general descent in height of the optical signature is consistent with the height variations of the EISCAT backscatter enhancements. These persistent ion line enhancements in the vicinity of the O-mode HF reflection altitude are the result of parametric decay of the pump electromagnetic wave in

vicinity of the O-mode reflection altitude into Langmuir and ion acoustic waves (Bernhardt et al., 1989; Stubbe et al., 1992; Djuth et al., 1994) and is commonly observed when pumping the ionosphere near an electron gyro-harmonic frequency (Kosch et al., 2004), e.g. 5.423 MHz corresponds to the 4th gyro-harmonic at 215 km altitude. The enhancements are only visible at angles close to the direction of the magnetic field line (Kosch et al., 2004). Therefore, in some of heater cycles there are no persistent ion line enhancements due to the radar look angle. The descent in altitude of the ion line data is a result of the descent of the pump wave's resonance region where the plasma frequency equals the pump frequency. Heating the lower F-layer plasma causes an increase in electron temperature (Rietveld et al., 2003) and decrease in electron recombination rate, thereby increasing the plasma density (Ashrafi et al., 2006). Electron density increases near the reflection point of the radio waves results in the descent of the reflection level of the pump wave.

The enhanced Langmuir waves accelerate electrons to supra-thermal velocities which then collide with the oxygen neutrals to produce 630.0 and 557.7 nm emissions. This is consistent with our height triangulation of the artificial optical emissions. The variation in height of the green line emission at 557.7 nm is similar to the temporal evolution in altitude of the ion line enhancements. The optical emission is being produced a few kilometers below the acceleration region, which is expected as the gas density increases at lower altitudes, making electron-neutral collisions more likely. The height difference between the ion-line enhancements and optical emissions on average is ~ 10 km, which is consistent with the night time mean free path between electron-atomic oxygen collisions of ~ 14 km at 210-220 km altitude (Gurevich, 1978).

The Ramfjordmoen camera was looking along the magnetic field line direction, therefore the recorded optical signature is the integration of all emissions distributed along the magnetic field line. This is because the optical aurora forms

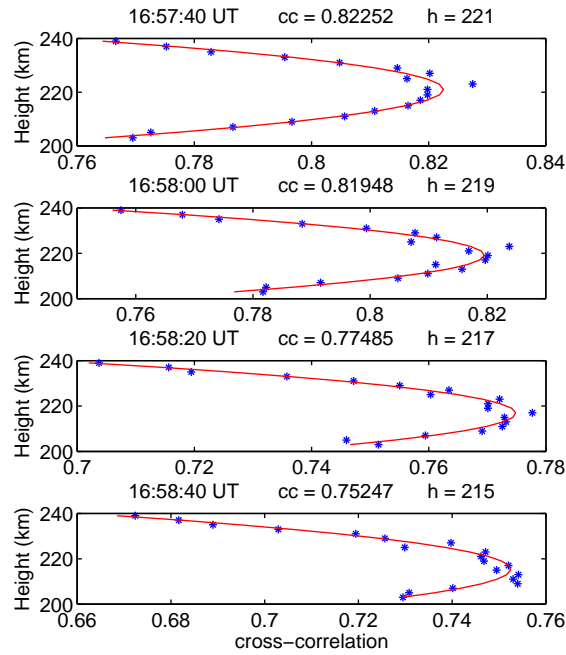


Fig. 3. The height vs. cross-correlation for the sequence of images with 20 seconds separation after the start of the Heater on cycle at 16:57:00 UT. The cross-correlation maximizes at a certain height for each time integration. The red curve indicates the 2nd order polynomial fit to the points, used to estimate the height of maximum cross-correlation. Time, maximum cross-correlation and the corresponding altitude are shown for each panel.

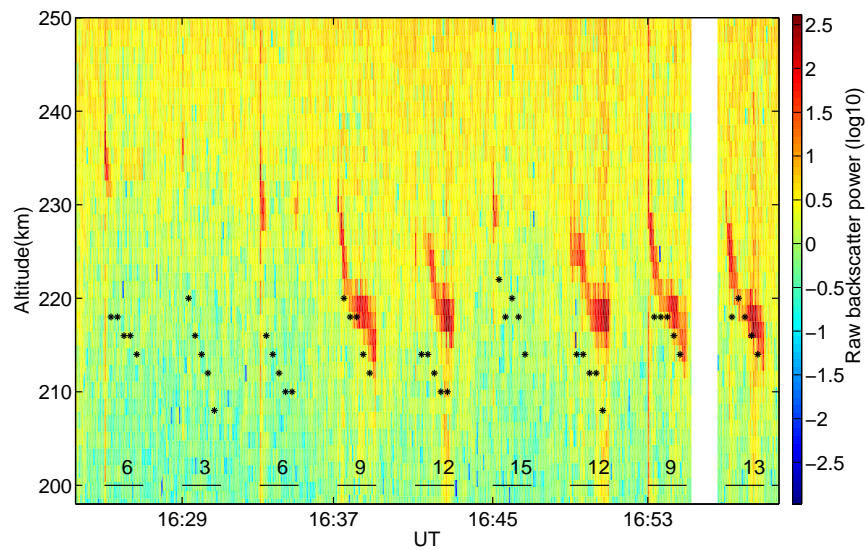


Fig. 4. Raw backscattered power from the EISCAT UHF radar shown in false color. The asterixes show the height triangulation of the optical artificial aurora at 557.7 nm. The intervals indicated by the lines are Heater on cycles and the labels are radar zenith angle south of vertical.

a cylinder above the pump wave reflection altitude parallel to the magnetic field line direction (Kosch et al., 2004). The apparent thickness of the partial ring in the Ramfjordmoen image is the real horizontal width of the structure. The DASI camera pointing towards local zenith ~ 50 km away recorded the column of artificial aurora at an oblique angle. This difference in the look directions leads to vertical extent ambiguity between the images from the two cameras and reduces the cross-correlation coefficient as a result. To properly estimate the vertical extent and altitude of the artificial aurora, a third camera would be needed, but this was not available at the time. The effect is visible in the DASI images where the optical ring recorded by DASI appears horizontally thicker compared to the Ramfjordmoen camera ring structure (Fig. 2). Using the apparent increased horizontal extension of optical signature in the DASI images compared to the Ramfjordmoen images, it is possible to estimate the vertical extent of the emission column by mapping the magnetic field line onto the images in geographic coordinates. For the example shown in Figure 2, the field aligned extension of the artificial aurora to first order is ~ 70 km which is consistent with Kosch et al. (2004).

References

- Ashrafi, M., Kosch, M. J., and Honary, F.: Heater-induced altitude descent of the EISCAT UHF ion line enhancements: observations and modelling, *Adv. Space Res.*, In press, 2006.
- Bernhardt, P. A., Duncan, L. M., and Tepley, C. A.: Artificial airglow excited by high-power radio waves, *Science*, 242, 1022–1027, 1988.
- Bernhardt, P. A., Tepley, C. A., and Duncan, L. M.: Airglow enhancements associated with plasma cavities formed during ionospheric heating experiments, *J. Geophys. Res.*, 94, 9071–9092, 1989.
- Bernhardt et al., P. A.: Excitation of artificial airglow by high power radio waves from the "SURA" ionospheric heating facility, *Geophys. Res. Lett.*, 18, 1477–1480, 1991.
- Brändström, B. U. E., Leyser, T. B., Steen, A., Rietveld, M. T., Gustavsson, B., Aso, T., and Ejiri, M.: Unambiguous evidence of HF pump-induced airglow at auroral latitudes, *Geophys. Res. Lett.*, 26, 3561, 1999.
- Djuth, F. T., Stubbe, P., Sulzer, M. P., Kohl, H., Rietveld, M. T., and Elder, J. H.: Altitude characteristics of plasma turbulence excited with the Tromsø superheater, *J. Geophys. Res.*, 99, 333–339, 1994.
- Duffet-Smith, P.: *Practical astronomy with your calculator*, Cambridge University Press, Cambridge, 1990.
- Gurevich, A. V.: *Nonlinear phenomena in the ionosphere*, Elsevier, North-Holland, 1978.
- Gustavsson, B., Sergienko, T., Rietveld, M. T., Honary, F., Steen, A., Brändström, B. U. E., Leyser, T. B., Aruliah, A. L., Aso, T., Ejiri, M., and Marple, S.: First tomographic estimate of volume distribution of HF-pump enhanced airglow emission, *J. Geophys. Res.*, 106, 29 105–29 124, 2001.
- Haslett, J. C. and McGill, L. R.: A model of enhanced airglow excited RF-radiation, *Radio Science*, 9, 1005–1019, 1974.
- Kosch, M. J., Rietveld, M. T., Hagfors, T., and Leyser, T. B.: High-latitude HF-induced airglow displaced equatorwards of the pump beam, *Geophys. Res. Lett.*, 27, 2817–2820, 2000.
- Kosch, M. J., Rietveld, M. T., Senior, A., McCrea, I., Kavanagh, A. J., Isham, B., and Honary, F.: Novel artificial optical annular structures in the high latitude ionosphere over EISCAT, *Geophys. Res. Lett.*, 31, L12 805, doi:10.1029/2004GL019713, 2004.
- Leyser, T. B., Gustavsson, B., Brändström, B. U. E., Honary, F., Å. Steen, Aso, T., Rietveld, M. T., and Ejiri, M.: Simultaneous measurements of high-frequency pump-enhanced airglow and ionospheric temperatures at auroral latitudes, *Adv. Polar Upper Atmos. Res.*, 14, 1–11, 2000.
- Pedersen, T. R. and Carlson, H. C.: First observations of HF heater produced airglow at the high frequency active aurora research program facility: Thermal excitation and spatial structuring, *Radio Sci.*, 36, 1013–1026, 2001.
- Rietveld, M. T., Kosch, M. J., Blagoveshchenskaya, N. F., Kornienko, V. A., Leyser, T. B., and Yeoman, T. K.: Ionospheric Electron Heating, Optical Emissions, and Striations Induced by Powerful HF Radio Waves at High Latitudes: Aspect Angle Dependence, *J. Geophys. Res.*, 108, 2/1–2/16,

doi:10.1029/2002JA009543, 2003.

Sipler, D. P., Enemark, E., and Biondi, M. A.: 6300-

A intensity variations produced by the Arecibo ionospheric modification experiment, *J. Geophys. Res.*, *77*, 4276–4280, 2001.

Störmer, C.: *The Polar Aurora*, Oxford University Press, London, 1955.

Stubbe, P., Kohl, H., and Rietveld, M. T.: Langmuir turbulence and ionospheric modification, *J. Geophys. Res.*, *97*, 6285–6297, 1992.